ARTICLE

Genetic manipulation of primary human natural killer cells to investigate the functional and oncogenic roles of PRDM1

Gehong Dong,[1,2*] Yuping Li,[1*] Logan Lee,[1] Xuxiang Liu,[1] Yunfei Shi,[1,3] Xiaoqian Liu,[1,4] Alyssa Bouska,[5] Qiang Gong,[1] Lingbo Kong,[1] Jinhui Wang,[6] Chih-Hong Lou,[7] Timothy W. McKeithan,[1] Javeed Iqbal[5] and Wing C. Chan[1]

[1]Department of Pathology, City of Hope National Medical Center, Duarte, CA, USA; [2]Department of Pathology, Beijing Tiantan Hospital, Capital Medical University, Beijing, China; [3]Department of Pathology, Peking University Cancer Hospital & Institute, Key Laboratory of Carcinogenesis and Translational Research (Ministry of Education), Beijing, China; [4]Department of Hematology, Affiliated Yantai Yuhuangding Hospital, Qingdao University, Yantai, Shandong, China; [5]Pathology and Microbiology, University of Nebraska Medical Center, Omaha, NE, USA; [6]Department of Molecular and Cellular Biology, City of Hope, Duarte, CA, USA and [7]The Gene Editing and Viral Vector Core, Department of Shared Resources, Beckman Research Institute of City of Hope, Duarte, CA, USA

**GD and YL contributed equally as co-first authors.*

Ferrata Storti Foundation

Haematologica 2021
Volume 106(9):2427-2438

ABSTRACT

Extra-nodal natural killer (NK)/T-cell lymphoma, nasal type (ENKTCL) is a highly aggressive lymphoma, in which the tumor suppressor gene *PRDM1* is frequently lost or inactivated. We employed two different CRISPR/Cas9 approaches to generate *PRDM1*$^{-/-}$ primary NK cells to study the role of this gene in NK-cell homeostasis. *PRDM1*$^{-/-}$ NK cells showed a marked increase in cloning efficiency, higher proliferation rate and less apoptosis compared with their wild-type counterparts. Gene expression profiling demonstrated a marked enrichment in pathways associated with proliferation, cell cycle, MYC, MYB and TCR/NK signaling in *PRDM1*$^{-/-}$ NK cells, but pathways associated with normal cellular functions including cytotoxic functions were down-regulated, suggesting that the loss of *PRDM1* shifted NK cells toward proliferation and survival rather than the performance of their normal functions. We were also able to further modify a *PRDM1*-deleted clone to introduce heterozygous deletions of common tumor suppressor genes in ENKTCL such as *TP53, DDX3X,* and *PTPN6*. We established an *in vitro* model to elucidate the major pathways through which *PRDM1* mediates its homeostatic control of NK cells. This approach can be applied to the study of other relevant genetic lesions and oncogenic collaborations in lymphoma pathogenesis.

Introduction

Extra-nodal natural killer (NK)/T-cell lymphoma, nasal type (ENKTCL) is a highly aggressive lymphoma that is consistently associated with Epstein-Barr virus (EBV) infection and predominantly affects middle-aged men in Asia and Central and South America.[1,2] It typically presents as tumors or destructive lesions in the nasal cavity, maxillary sinuses or palate. Despite a localized presentation in most patients, it tends to relapse locally or at other extra-nodal sites, such as the skin, and the 5-year overall survival of affected individuals is 40-50% with current therapeutic regimens.[2,3] About 80-90% of ENKTCL originate from the NK-cell lineage with the rest of cases derived from T cells. Regardless of the cell of origin, the pathology, clinical behavior and treatment are similar. Aggressive NK-cell leukemia, also EBV-associated and derived from NK cells, is regarded as the leukemic form of ENKTCL.[4]

Our previous genomic analysis of ENKTCL,[5,6] including identification of copy number abnormalities, mutation analysis, and DNA methylation studies, suggested that *PRDM1*, located in 6q21, is a tumor suppressor gene that is frequently inactivat-

Correspondence:

WING C. (JOHN) CHAN
jochan@coh.org

Received: April 8, 2020.
Accepted: July 30, 2020.
Pre-published: July 30, 2020.

https://doi.org/10.3324/haematol.2020.254276

ed by deletion, methylation and mutation. The minimal common region of the 6q21 deletion contains a number of genes (*ATG1, AIM1*, etc.) but apart from *PRDM1*, they have not been found to be mutated or methylated either by us or others. We therefore prioritized *PRDM1* for further study, and functional analysis of the gene supports its role as a tumor suppressor gene.[6-8] *PRDM1* has also proven to be a tumor suppressor gene in diffuse large B-cell lymphomas[4] and anaplastic large T-cell lymphoma.[9] Accumulating evidence supports the concept that it is not only critical for terminal effector cell differentiation in B cells[10] but that it is also important in the homeostasis of T cells and in T-cell[4] effector differentiation. The level of PRDM1 increased progressively with NK-cell activation with a corresponding drop in MYC level, termination of proliferation and increased cellular apoptosis.[6] The precise role of PRDM1 in this process is not clear, and the inability to maintain human NK cells in long-term culture *in vitro* with interleukin (IL)-2 or IL-15 is a major impediment to further analysis. We are now able to perform long-term *in vitro* cultures of primary, normal NK cells which allow sufficient time for us to perform specific genetic manipulations and functional studies with genome-edited cells and single-cell clones using the recently developed clustered regularly interspaced short palindromic repeat (CRISPR)/CRISPR-associated protein 9 (Cas9) system for targeted gene editing.[11] Here, we report the functional consequences of *PRDM1* gene knock-out (KO) in primary NK cells from healthy donors and the implication of these findings on NK-cell homeostasis and ENKTCL pathogenesis.

While *PRDM1* is a frequently mutated tumor suppressor gene in NK-cell lymphomagenesis,[6-8] it is not sufficient by itself to generate a lymphoma in a murine model, and additional alterations are necessary. As many of the frequent genetic and epigenetic changes in ENKTCL are loss-of-function alterations, the CRISPR/Cas 9 system enables highly efficient targeted gene editing[11] to investigate these abnormalities.[12-16] Here, we demonstrated other potential tumor suppressor genes that are readily modified and the feasibility of inducing pairs of deletions to study cooperative mutations in NK-cell lymphomagenesis.

Methods

Primary NK-cell enrichment

Primary NK cells were isolated from peripheral blood mononuclear cells of healthy donors (donor #1 and donor #2) using the EasySep™ Human NK Cell Enrichment Kit (Stemcell, USA; #19055) according to the manufacturer's protocol. The purity of isolated NK cells was determined by flow cytometry analysis with FITC-labeled anti-human CD56 (Biolegend, USA; n. 362545) and PE-labeled anti-human CD3 (Biolegend, USA, n. 300407) double staining.

PRDM1 knockout mediated by CRISPR/Cas9 with plasmid PX458-sgRNA4

The PX458-sgRNA4 plasmid was delivered into stimulated primary NK cells by electroporation using the Amaxa® Nucleofector® II Device (Lonza, France) according to the manufacturer's suggested U001 protocol (5 μg plasmid per $2x10^6$ cells) (Figure 1A). Cloning of the modified cells is described in the *Online Supplementary Methods*. Sequential gene KO was processed similarly but on identified *PRDM1*$^{-/-}$ NK clone #3. The various guide RNA used in these experiments are listed in *Online Supplementary Tables S1* and *S2*.

CRISPR/Cas9-mediated disruption of *PRDM1* by introduction of a fluorescent protein through homologous recombination

Cas9/sgRNA ribonucleoprotein (RNP) complexes targeting *PRDM1* exon 5 (Figure 1B), together with a double-stranded DNA repairing template consisting of a fluorescent protein gene (GFP/DsRed) flanked by long homologous arms of the *PRDM1* gene, were electroporated into cells, allowing the edited cells, of which both *PRDM1* loci were disrupted, to be sorted by fluorescence activated cell sorting (FACS). Details of the experiment are shown in *Online Supplementary Figure S1* and Figure 1B. sgRNA2 used in this experiment is shown in *Online Supplementary Table S1*.

Other experimental methods

Cell lines used and cell culture methods, the CRISPR/Cas9 experiments, western blotting, cell proliferation and apoptosis assays, cell cycle analysis, quantitative real-time polymerase (qRT-PCR), RNA-sequencing, next-generation sequencing, and statistical analysis, are described in the *Online Supplementary Information*.

Results

Generation of *PRDM1*$^{-/-}$ primary NK cells by two different CRISPR/Cas9 methods

Generation of PRDM1$^{-/-}$ *clones #3 and #5 using PX458-sgRNA4 plasmid electroporation*

With our feeder cell culture system, we successfully cloned primary NK cells after single-cell seeding by FACS. The expanded NK-cell single clones (G-2 and G-3) were observed for approximately 3 weeks (*Online Supplementary Figure S2*) and were enumerated for evaluation of cloning efficiency. According to our grading system, as specified in the Methods section, the GFP$^+$ cells (plasmid-transfected cells) had significantly higher cloning efficiency (47.7% *vs.* 11.7%; $P<0.05$) than parental primary NK cells (*Online Supplementary Table S3*). Sequencing analysis revealed that 66% (61 of 92) of the clones showed *PRDM1* frame-shift deletions around the target site within exon 4 (*Online Supplementary Figure S3*), with the likelihood of their having been four founders based on the pattern of deletions. Two of these four founder clones with distinct homozygous deletions (Figure 2A, B) were the most prevalent clones isolated by single-cell cloning, indicating that homozygous deletion of *PRDM1* confers a growth advantage among these clones. Clones #3 and #5 belonged to one of the homozygous deletions and were chosen as the biological duplicates in our subsequent studies. The loss of *PRDM1* protein expression was confirmed by western blot analysis in these clones (Figure 2C, upper panel). We also measured the expression of the PRDM1 target gene *MYC* in the edited cells and demonstrated that the expression of *MYC* was upregulated (9-fold) upon *PRDM1* KO (Figure 2C, lower panel).

Generation of bulk PRDM1$^{-/-}$ *NK cells through fluorescent protein knock-in by homologous DNA repair using Cas9/sgRNA2 ribonucleoprotein electroporation*

To avoid the selection process inherent in cloning and potential spurious results due to off-target modification by sgRNA4, we modified a recently described technology

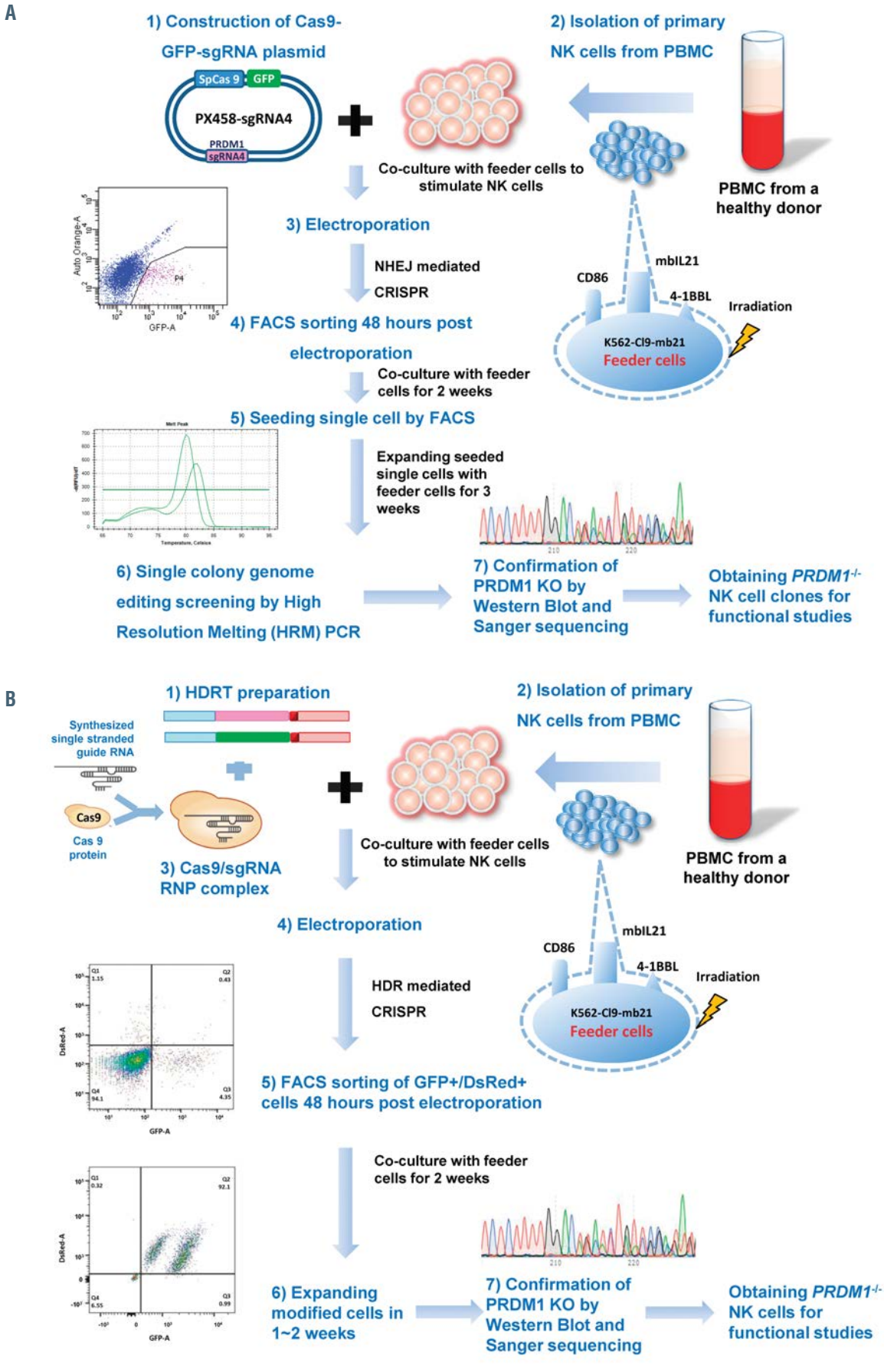

Figure 1. Legend on following page.

Figure 1. Schematic diagram of knock-out of *PRDM1* in NK cells by the CRISPR/Cas9 system. (A) *PRDM1* was knocked out by using a Cas9-sgRNA plasmid. The plasmid with both Cas9-GFP and sgRNA is shown. This approach requires cloning of GFP$^+$ NK cells on irradiated feeder cells. Genome editing was evaluated by a high resolution melting-polymerase chain reaction assay and the *PRDM1* knock-out was confirmed by western blot and Sanger sequencing. (B) *PRDM1* was knocked out by electroporation of the Cas9/sgRNA RNP complex plus a homology directed repair (HDR) template with fluorescence protein gene. Double-stranded HDR DNA templates with inserted GFP or DsRed open reading frame and about 300 bp homologous sequence of exon 5 at each side of the CRISPR/Cas9 cutting site of sgRNA2 were prepared. FACS for GFP and DsRed double positive cells identified *PRDM1* knock-out cells, which were confirmed by western blot and Sanger sequencing. Cas9: CRISPR-associated protein 9; GFP: green fluorescent protein; NK: natural killer; PBMC: peripheral blood mononuclear cells; NHEJ: non-homologous end joining; CRISPR: clustered regularly interspaced short palindromic repeat; FACS: fluorescence activated cell sorting; PCR: polymerase chain reaction; KO: knock-out; HDRT: homology directed repair template; RNP: ribonucleoprotein.

developed for primary T-cell CRISPR editing[17] for our primary NK-cell genome editing. We chose another guide RNA for exon 5, sgRNA2 (*Online Supplementary Table S1*, Figure 3A). A homologous DNA repair (HDR) template encompassing an in-frame fusion of either GFP or DsRed open reading frame followed by a strong stop signal from SV40 poly (A) tail was included (Figure 3B, *Online Supplementary Figure S1*). This approach utilized HDR that introduced GFP or DsRed as markers of a disrupted *PRDM1* locus. Cells with two colors indicated bi-allelic insertion of the fluorescent protein and the termination of *PRDM1* expression and could be FACS-sorted (Figure 1B).

After expansion of the GFP$^+$/DsRed$^+$ double-positive NK cells, we performed genotyping, qRT-PCR and western blot to confirm the bi-allelic *PRDM1* KO (Figures 3C and 4A-C, *Online Supplementary Table S4*). The low PRDM1 expression remaining in qRT-PCR (Figure 4C) and western blotting of *PRDM1*$^{-/-}$ NK cells (Figure 3C) was from the contaminating feeder cells (*Online Supplementary Figure S4*). When we used the *PRDM1* primers located in exon 2 and exon 3, upstream of the sgRNA2 cutting site, to perform qRT-PCR, a high level of expression was observed. As PRDM1 is an autologous repressor, the upregulation of *PRDM1* transcripts upstream of the truncation should not be a surprise and is consistent with earlier observations (Figure 4D). *MYC* transcription was upregulated in these cells (Figure 3C). These results indicate that we had developed a separate method of generating *PRDM1*$^{-/-}$ NK cells.

PRDM1$^{-/-}$ NK cells showed growth advantage compared with normal wild type NK cells

PRDM1$^{-/-}$ *NK cells had a growth advantage*

As shown in Figure 5A, the *PRDM1*$^{-/-}$ NK clones #3 and #5 had higher growth rates (>2 fold) compared with their normal wild-type (WT) counterparts as measured by an MTS assay. A similar effect was observed with GFP$^+$/DsRed$^+$ *PRDM1*$^{-/-}$ NK cells (Figure 5B). In fact, the GFP$^+$/DsRed$^+$ *PRDM1*$^{-/-}$ NK cells grew even better than clones #3 and #5 and expanded 4.2-fold in 6 days, while the WT NK cells expanded less than 2-fold. It must be noted that the GFP$^+$/DsRed$^+$ *PRDM1*$^{-/-}$ NK cells were relatively younger (~20 days after CRISPR), whereas clone #3 and clone #5 were examined ~90 days after CRISPR. A steady decline in growth rate was observed in *PRDM1*$^{-/-}$ cells after long-term *in vitro* culture.

PRDM1$^{-/-}$ *NK cells had an increased fraction of cells in the S/G2M phase*

We performed cell cycle analysis on *PRDM1*$^{-/-}$ NK cells (clone #3 and clone #5) at around 90 days of culture, and cells undergoing DNA synthesis were measured by EdU incorporation into DNA for 5 consecutive days. Remarkably, 40% of the *PRDM1*$^{-/-}$ NK cells were in the S/G2M phase *versus* ~4% in WT NK cells (Figure 5C, D) on the 3rd day after adding fresh feeder cells. This proliferation was feeder-dependent, as the proliferating rates were reduced after feeder cells had all died (Figure 5D), but the *PRDM1*$^{-/-}$ clones demonstrated a more sustained proliferation. As observed on the 7th day, >20% of the total *PRDM1*$^{-/-}$ cells showed EdU incorporation (decreased about 1.5-fold), whereas 1% of the parental cells showed EdU incorporation. Similar results were obtained with GFP$^+$/DsRed$^+$ *PRDM1*$^{-/-}$ NK cells. The proportion of EdU-positive cells in *PRDM1*$^{-/-}$ NK cells was 44.2% on the 3rd day and 17.8% on the 7th day (~2.5-fold drop), whereas the proportions of EdU-positive WT NK cells were 23.7% on the 3rd day and 4.75% on the 7th day (~5-fold drop) (Figure 5E). These results indicated that, compared with WT NK cells, *PRDM1*$^{-/-}$ NK cells had a higher rate of proliferation and a more sustained response to feeders, in agreement with the findings from *PRDM1*$^{-/-}$ clones #3 and #5. These results indicated that PRDM1 regulates cell proliferation and longevity in the presence of feeder cell stimulation.

We also performed cell cycle analysis and observed that a higher proportion of *PRDM1*$^{-/-}$ NK cells were in the S/G2M phase (22.9~28.5%) compared with WT control cells (18.7%) (Figure 6D). Similar results were obtained with GFP$^+$/DsRed$^+$ *PRDM1*$^{-/-}$ NK cells, of which 26.4% were in S/G2M phase *versus* the 17.0% of WT NK cells in the S/G2M phase (Figure 5F). Moreover, in both groups of NK cells, we found there was a slightly higher ratio of the S phase cell fractions (1.5~2.2-fold) in *PRDM1*$^{-/-}$ NK cells than in WT NK cells. These results unequivocally demonstrated that PRDM1 regulates cell proliferation and growth in NK cells.

PRDM1$^{-/-}$ *primary NK cells had fewer apoptotic cells*

Consistent with the above analysis, there were fewer early apoptotic cells (Q3) in *PRDM1*$^{-/-}$ clones #3 and #5 than WT NK cells at different days of observation after adding fresh feeder cells (Figure 6A). Statistical analysis showed the general trend of increase of early apoptotic cells in both *PRDM1*$^{-/-}$ and WT NK cells after feeder cell stimulation (Figure 6B). This observation paralleled the decrease in growth and proliferation of the cells. It is possible that as the cells entered a more quiescent phase, apoptosis also decreased. Similar results of fewer early apoptotic cells in *PRDM1*$^{-/-}$ NK cells compared with their WT counterpart were obtained with GFP$^+$/DsRed$^+$ *PRDM1*$^{-/-}$ NK cells (Figure 6C). However, the percentages of early apoptotic cells (Q3) tended to get lower, not higher, with the days in culture with feeder cells. This may be due to the fact that the cells in the second batch were at a relative earlier phase of their lifespan than the single clones #3 and #5, so the cells responded better to the feeder cell stimulation.

Generation of dual-gene knockout NK cells and off-target evaluation

Other than single-gene KO, we also introduced deletions in genes often deleted or mutated in NK-cell lymphomas (e.g. *TP53, DDX3X* and *PTPN6*). We obtained several different dual-gene KO NK cells using the pSpCas9(BB)-2A-

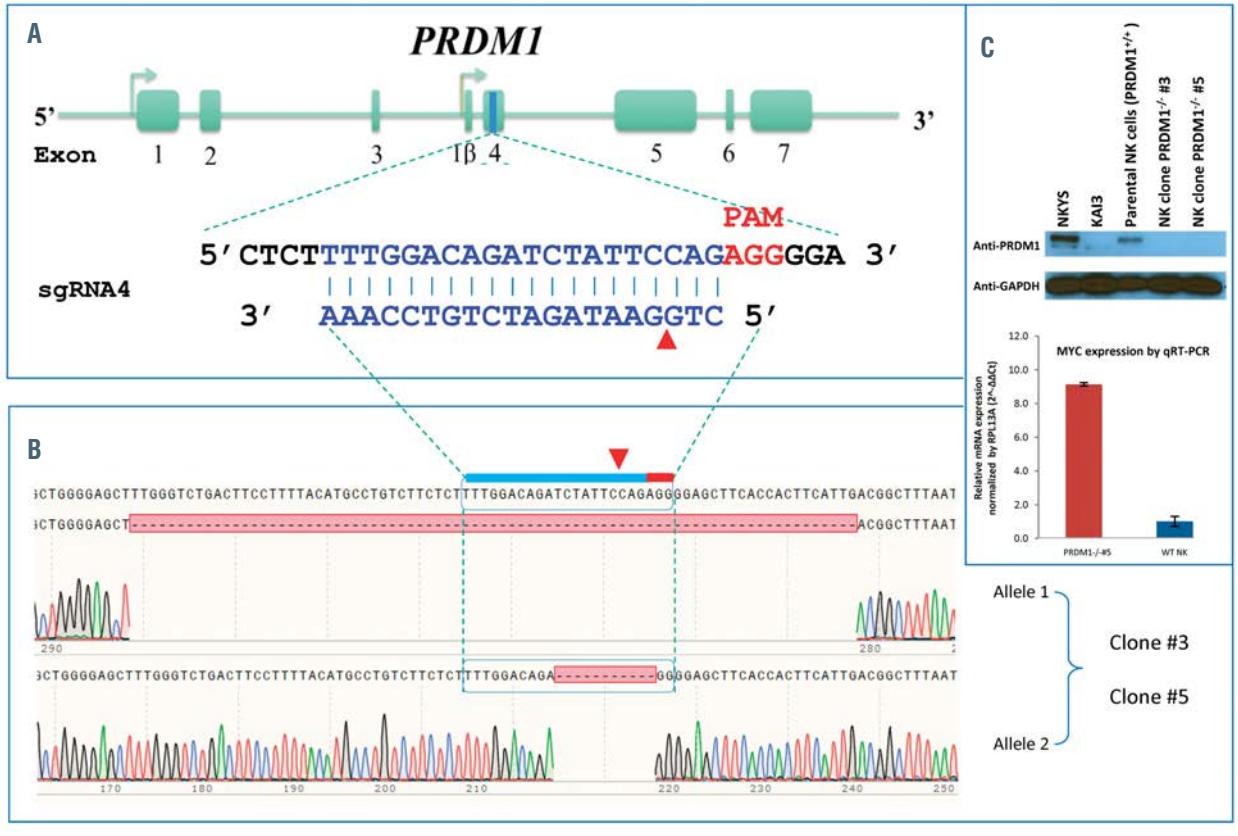

Figure 2. Sanger sequencing demonstrating the *PRDM1* deletion in clones #3 and #5. (A) Guide RNA sgRNA4 sequence and schematic gene structure of *PRDM1*. Light green boxes and numbers represent the exons of the *PRDM1* gene. (B) TOPO cloning showed that both clones #3 and #5 harbored the same bi-allelic deletion, a 79-bp deletion in one allele (comprising 35 bp from exon 4 [411-445] and 44 bp from the adjacent intron 3 and a 11-bp deletion in the other allele (413-424) (Ref: NM_001198). (C) Western blot analysis of PRDM1 protein in clones #3 and #5 (upper panel). Parental wild-type natural killer (NK) cells were used as a positive control. NK lymphoma cell lines, NKYS and KAI3, were used as positive and negative controls, respectively. PRDM1 target gene MYC expression of *PRDM1*$^{-/-}$ clone #5 versus wild-type NK cells was measured by quantitative reverse transcription polymerase chain reaction (qRT-PCR) (lower panel). The target gene expression levels were normalized to RPL13A, and relative expression was calculated using the 2^-ΔΔCt method. The expression of MYC in WT NK cells was set at 1.0.

GFP plasmid vector based approach[18] on *PRDM1*$^{-/-}$ NK clone #3 (*Online Supplementary Figures S5-S7*). All the double modified cells we obtained harbored heterozygous deletions of the second targeted gene, *TP53, DDX3X* or *PTPN6*. There were no major changes in cellular characteristics or cloning efficiency despite the loss of additional tumor suppressor genes, suggesting that heterozygous deletion of these tumor suppressor genes did not provide additional growth or proliferation advantage to NK cells with *PRDM1* deletion.

To evaluate whether the observed changes could be largely due to off-target effects from CRISPR/Cas9 gene editing, we performed custom capture and sequencing of known driver mutations in lymphoma using a panel of 334 genes (*Online Supplementary Table S5*) but did not observe any mutations or copy number abnormalities in *PRDM1*-edited clones compared with the WT counterpart. Thus, the changes observed in *PRDM1*$^{-/-}$ cells were not due to alterations of the exomes of any of the genes tested in the panel (334 genes).

Gene expression analysis of *PRDM1* knockout cells

To elucidate the functional alterations resulting from *PRDM1* deletion, we performed RNA-sequencing analysis on *PRDM1*-deficient NK cells or clones and cell-age-matched WT NK cells from the same donors, including two biological replicates. We were able to detect the deletion of exon 4 sequences and insertion of the GFP sequence in the RNA-sequencing analysis (*Online Supplementary Figure S8A-C*), thus disrupting the *PRDM1* open reading frame. The truncated mRNA in *PRDM1*$^{-/-}$ clones were transcribed at higher levels (>2-fold) compared with their WT counterparts, likely due to loss of negative autoregulation by PRDM1. As shown in *Online Supplementary Figure S8A*, these truncated mRNA did not result in any PRDM1 protein expression. Initial analysis using hierarchical clustering suggested that clusters were partly driven by distinct donor profiles and that *PRDM1*$^{-/-}$ clones tended to form tight clusters (Figure 7A). Approximately 30% (3,684 of 12,633) of transcripts were differentially expressed (1,419 downregulated, 1,498 upregulated; $P<0.05$ and false discovery rate <0.3) (Figure 7B). As anticipated, numerous genes and pathways associated with proliferation and cell cycle regulation and progression (e.g., cell cycle control, chromosomal replication, centrosome maturation, RNA splicing, DNA repair, S-phase and G2/M transition targets, E2F targets, MYC, IRF4, E2F3 induction) were upregulated/enriched in the *PRDM1*-deleted clones (Figure 7C).

Genes regulated by the DREAM complex (Dimerization partner, RB-like, E2F4 and multi-vulval class B, master coordinator of cell cycle-dependent gene expression) were enriched upon *PRDM1* loss, suggesting that the DREAM repressor complex converts into an activating complex in the absence of *PRDM1*. Metabolic changes, such as glycogen metabolism, also showed enrichment in *PRDM1*$^{-/-}$ NK cells. Various genes associated with NK-cell biology (*TOX2,*

TLR4,[19] *CCR4*,[20] *VEGF*,[21] *TP63* and *IRF4*) were upregulated >20-fold in *PRDM1*$^{-/-}$ cells (*Online Supplementary Figure S8D*). TOX2 is a critical transcription factor for NK-cell maturation/development upstream of T-bet/TBX21, suggesting that PRDM1 may regulate NK-cell development and function via TOX2.[22] Similar to a previous study in mouse NK cells, there was a marked increase in the expression of IRF4 and its target genes upon *PRDM1* KO.[23] In contrast to the *PRDM1* KO cells, the WT cells showed enrichment of genes associated with the FOXO3 pathway, TP53/63, and NK-cell-mediated cytotoxicity (*Online Supplementary Figure S8E*). Several gene signatures associated with endosomal sorting, lysosomes and secretion, and cell-to-cell communication (e.g., E-cadherin stabilization) were enriched in these cells. Other than these, gene sets associated with quiescence and IL-12, P38 MAPK and TNFR1 signaling were also enriched (Figure 7D). The genes that were downregulated included T-cell and NK-cell signaling and KIR3DL1-3 or KIR3DL members, which generally transduce inhibitory signals upon ligand binding (*Online Supplementary Figure S8F*). A recent report indicated that several immune checkpoint molecules in CD8^{+} T cells,[24] including LAG-3, are upregulated by PRDM1 alone or in combination with MAF. We examined our data and found that the co-inhibitory receptors/molecules LAG3, LILRB1, LILRB3, and CD244 were downregulated in *PRDM1*$^{-/-}$ cells, which may thus impair immune checkpoints in NK cells similarly to cytotoxic T-cells.

We performed qRT-PCR on selected transcripts based on their significant alteration on RNA-sequencing and their potentially important biological functions, comparing LAG3, GNLY, PRF1, TOX2 and CCR4 expression in bulk donor #2 NK *PRDM1*$^{-/-}$ cells *versus* donor #2 NK WT cells. The qRT-PCR results were concordant with our RNA-sequencing results with higher levels of TOX2 and CCR4 and lower levels of LAG3, GNLY and PRF1 in *PRDM1*$^{-/-}$ cells (*Online Supplementary Figure S8G*). Furthermore, flow analysis indicated a concordant decrease in LAG3 protein expression in NK *PRDM1*$^{-/-}$ cells (*Online Supplementary Figure S8H*).

Discussion

We and other groups have identified several frequent mutations in ENKTCL, including a number of potential tumor suppressor genes such as *PRDM1, TP53, DDX3X* and *BCOR*.[5-8,25-27] We also found that ENKTCL has a marked DNA hypermethylation phenotype with inactivation of multiple tumor suppressors through this mechanism.[5] Some of the tumor suppressor genes are inactivated by a combination of genetic and epigenetic mechanisms, including *PRDM1* and *DDX3X*. The most common activating mutations involve the *JAK/STAT3* pathway, affecting ~20-30% of cases.[15,16] This may be related to the critical dependence of NK cells on IL-2 or IL-15, which signal through STAT3, STAT5A and STAT5B.[25] Interestingly, there is frequent DNA methylation of *PTPN6 (SHP1)*, a negative regulator of STAT3 and NK-cell receptor activation.[28-32] As *PRDM1* is a commonly inactivated tumor suppressor gene in ENKTCL, and as there is good evidence that PRDM1 regulates normal NK-cell as well as T-cell homeostasis,[6,26] we therefore focused on *PRDM1* deletion to elucidate the functions of PRDM1 in normal NK cells and how these relate to its tumor suppressor function.

The major challenge in deciphering the role of a genetic aberration in the pathogenesis of a lymphoma is the fre-

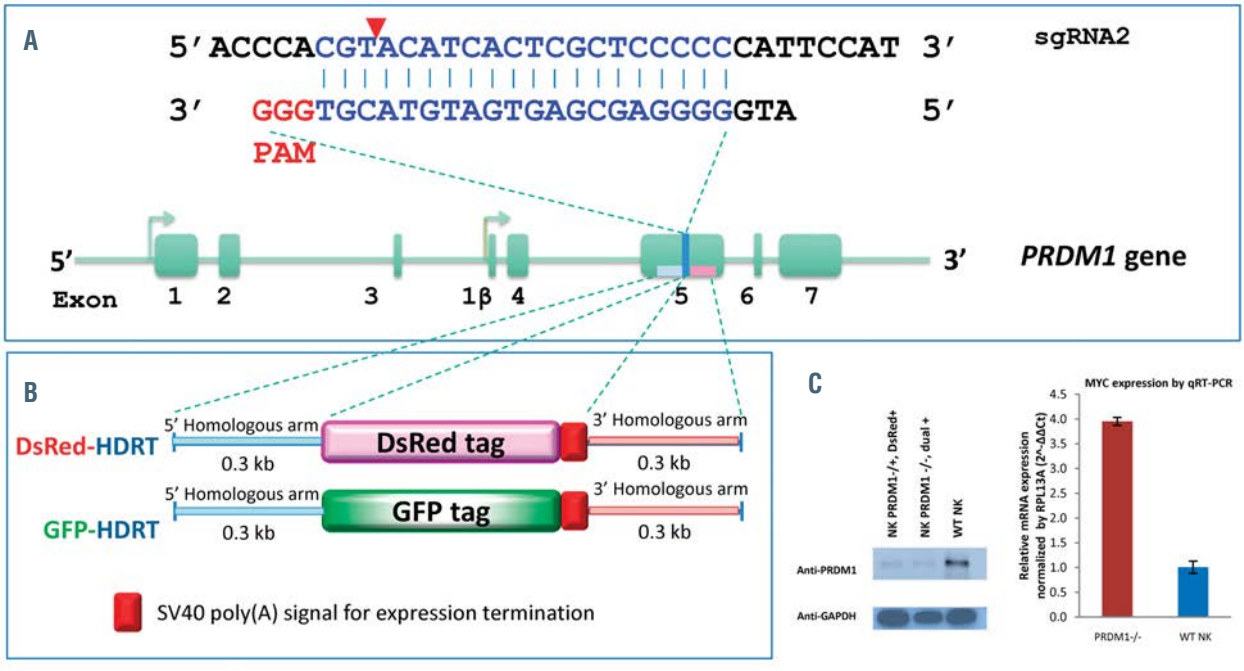

Figure 3. Schematic illustration of CRISPR/Cas9-mediated insertion of GFP or DsRed fusion tag to *PRDM1* exon 5 through a homology directed repair template to induce early termination of *PRDM1* expression. (A) Guide RNA sgRNA2 sequence and schematic gene structure of *PRDM1*. Light green boxes and numbers represent the exons of the *PRDM1* gene. The sequence of guide RNA sgRNA2 used for the homology directed repair (HDR) template-mediated CRISPR/Cas9 is shown above. (B) HDR templates were assembled with fluorescent tag GFP or DsRed open reading frame and a SV40 virus transcriptional stop signal (red box) in exon 5. (C) Western blot analysis of PRDM1 protein expression in *PRDM1*$^{-/-}$ NK cells and wild-type control cells (left panel). PRDM1 target gene *MYC* expression was measured by quantitative reverse transcription polymerase chain reaction (right panel). Target gene normalization and relative expression levels were determined as described in Figure 2.

quent presence of a large number of genetic and epigenetic changes in an established tumor as well as tumor heterogeneity. In addition, gene expression studies of the bulk tumor contain signals from the stromal elements as well as the tumor cells. We decided to develop an approach to study selected lesions in the normal cellular counterpart of the tumor, thereby determining the precise functional alteration induced by a single lesion or a known combination of lesions. A prerequisite of this approach in studying NK-cell lymphoma is the ability to grow human NK cells *in vitro* for a sufficiently long time to allow genetic manipulation and functional studies. Normal primary NK cells have a limited lifespan *in vitro*, but these cells can grow for >3 months with a feeder cell line (modified K562 cell line) and IL-2, thus allowing for genetic manipulations, selection and characterization of the mutants *in vitro*.

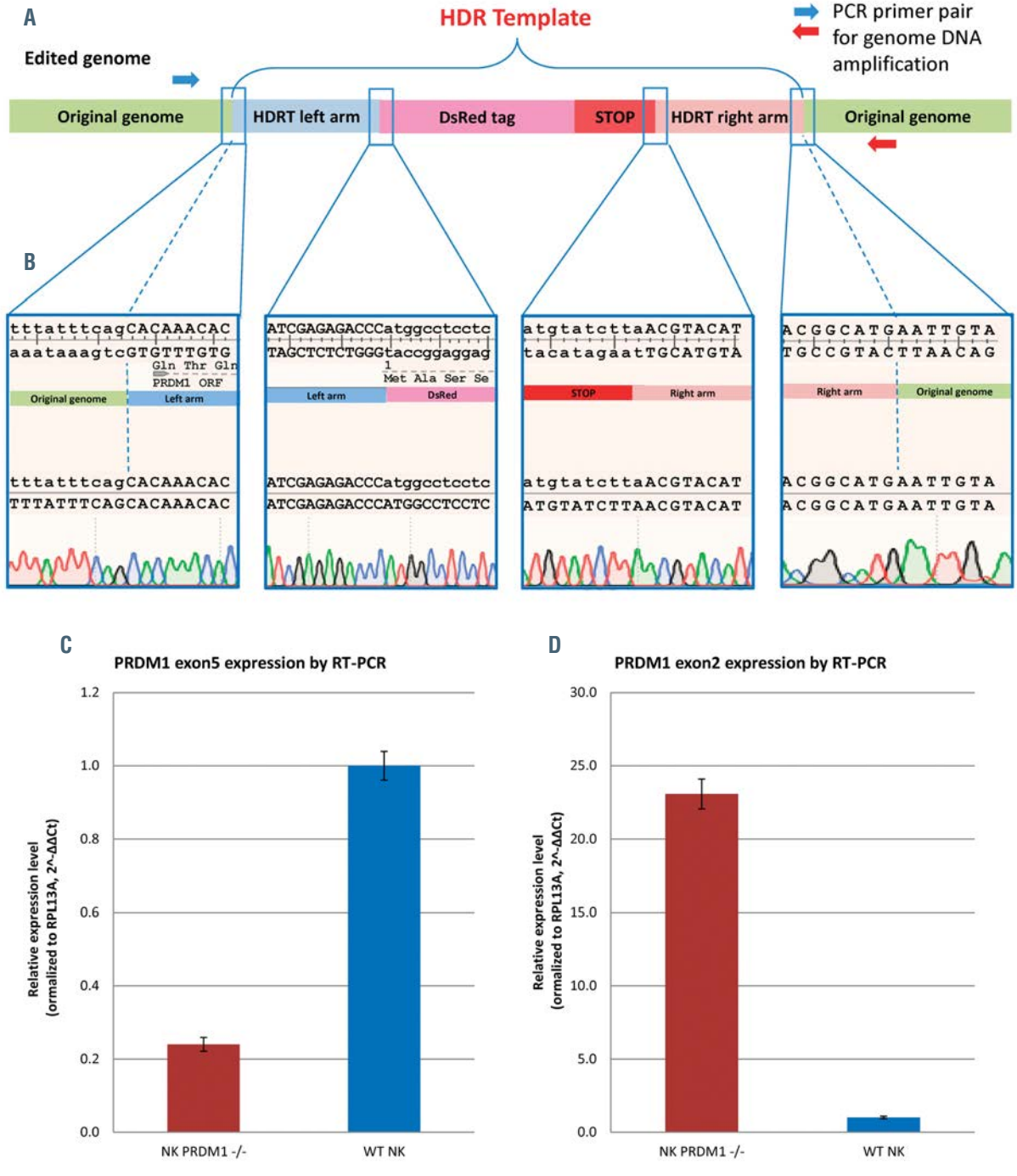

Figure 4. Sanger sequencing of the edited region of the *PRDM1* locus. . (A) The diagram shows the expected homology directed repair (HDR) template inserted into the *PRDM1* locus. (B) The DsRed reading frame, followed by the SV40 stop signal, was inserted in-frame into the *PRDM1* gene locus. The enlarged boxes show the junctional sequence between each adjacent fragment. Blue and red arrows indicate the primer pair located outside of the HDR template area to amplify the genome DNA fragment for Sanger sequencing. (C, D) Relative PRDM1 transcript levels of exon 5 and exon 2 in *PRDM1*$^{-/-}$ NK cells versus wild-type NK cells were measured by quantitative reverse transcription polymerase chain reaction (RT-PCR) and normalized to *RPL13A*. The expression levels were calculated by the 2^-ΔΔCt method, and *PRDM1* expression level in wild-type NK cells was set at 1.0.

We identified the tumor suppressor function of *PRDM1* in NK cells by knocking down *PRDM1* by shRNA transduction.[6] The recent development of CRISPR/Cas9 technology provides a powerful and versatile approach to edit the genome, thereby facilitating our understanding of the functional alterations induced by specific genetic alterations. Gene inactivation by methylation or mutation can be simulated by introducing small out-of-frame indels or knocking-in mutations. We were able to successfully KO selected tumor suppressor genes identified in ENKTCL, including mono-allelic and bi-allelic deletions. KO experiments rely on non-homologous end joining mechanisms and are very robust, but in the absence of a readily selectable marker, we have to rely on cloning to select for modified cells. This is a long and demanding process and may introduce a selection bias. Therefore, we adopted another approach to knock-in a fluorescent protein gene to disrupt the *PRDM1* locus while introducing a marker for selection. We were able to knock-in a GFP or DsRed gene into the *PRDM1* locus through HDR so that mono- or bi-allelic KO cells could be identified by single or double fluorescence, respectively. This approach shortened the experimental time and generated a bulk population of *PRDM1*$^{-/-}$ cells to complement and validate the observations from the cloning approach.

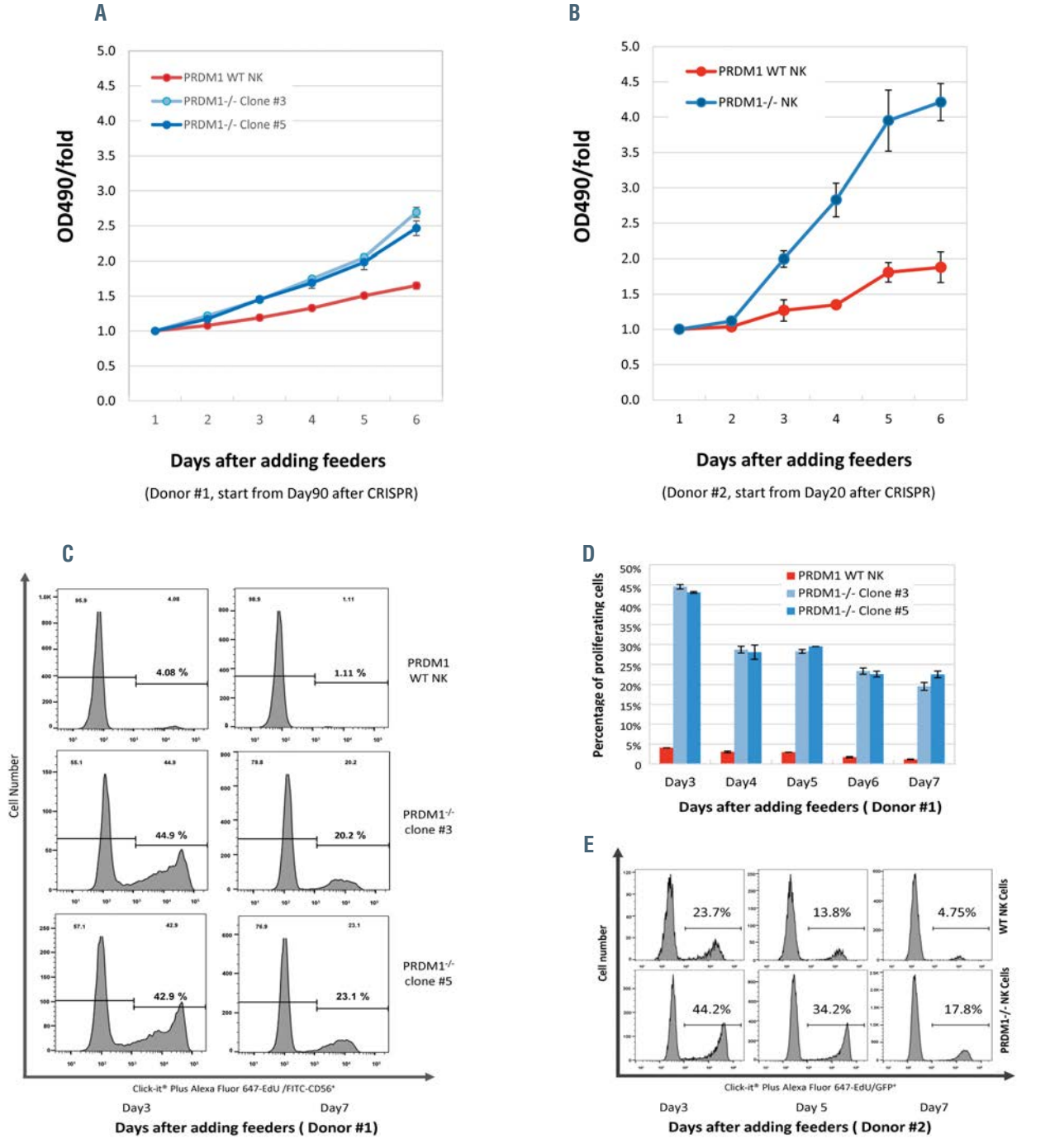

Figure 5. Figure continued on following page.

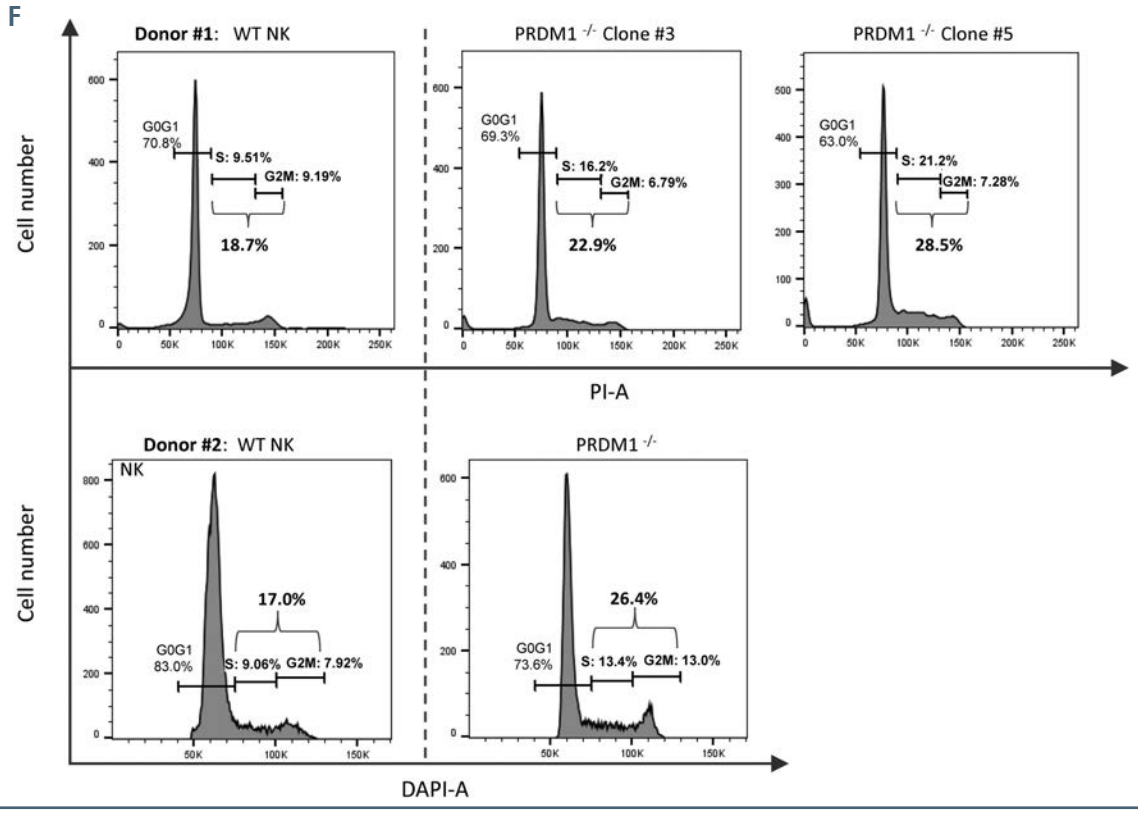

Figure 5. Proliferation and cell cycle distribution of *PRDM1*$^{-/-}$ NK cells *versus* wild-type NK cells. Cell growth analysis was measured by CellTiter 96® AQueous One Solution. The growth curve shows the relative fold-change of OD490 compared to the first day. (A) *PRDM1* was knocked out in NK cells (donor #1) using a Cas9-sgRNA plasmid. (B) *PRDM1* was knocked out of NK cells (donor #2) by Cas9/sgRNA ribonucleoprotein (RNP) and homology directed repair template (HDRT) electroporation. Cell proliferation was analyzed with the Click-iT™ Alexa Fluor 647-EdU Flow Cytometry assay during 5 consecutive days starting from the third day after fresh irradiated feeder cells had been added. (C) Flow analysis of clones #3 and #5 on day 3 and day 7 and donor #2 cells. FITC anti-CD56 antibody was used to identify NK cells. (D) Each staining of Alexa Fluor 647-EdU was performed in duplicate, and the figure shows the average. (E) Flow analysis of EdU assay on NK cells (donor #2). GFP positivity (for *PRDM1*$^{-/-}$ cells). (F) Cell cycle distribution was analyzed by cell DNA content staining with propidium iodide/RNase or DAPI with flow cytometric assay at the third day after fresh feeder cells had been added. The percentage of cells in each phase is shown in each box. Upper panel: corresponding WT cells and *PRDM1* knocked-out cells produced using the Cas9-sgRNA plasmid method. Lower panel: corresponding WT cells and *PRDM1* knocked-out cells produced using the Cas9/sgRNA RNP and HDRT method.

We were able to generate multiple homozygous *PRDM1* KO clones from different donors and demonstrated that *PRDM1* KO cells had a much higher cloning efficiency, a faster growth rate and a higher percentage of cycling cells than WT cells. There was also a modest reduction in apoptosis. The KO cells were also able to maintain their growth and proliferation for a longer period *in vitro*. These observations were largely validated using the bulk population of *PRDM1* KO cells, although there were some differences, which may have been related to the age of the cells in culture. When experiments were performed with younger cells, they exhibited higher growth and proliferation potentials. These observations suggested that PRDM1 is a key negative regulator of NK cells, and removing this control allows a striking increase in cloning efficiency, proliferation, growth and lifespan. This corroborated our previous observations[6] that primary NK cells could proliferate better with shRNA knock-down of *PRDM1*, and that the reconstitution of PRDM1 through retroviral transduction into a *PRDM1*-deficient NK-cell lymphoma line (KHYG) was associated with G2/M arrest, increased apoptosis and a strong negative selection pressure. This again strongly supports our findings that knock-out of *PRDM1* by CRISPR/Cas9 in primary NK promotes cell proliferation. In PRDM1 function rescue experiments, the rate of cell growth of pMIG-*PRDM1* electroporated NK *PRDM1* KO cells was significantly repressed compared to that of cells electroporated with empty vector (*Online Supplementary Figure S9*). Thus, elimination of *PRDM1* likely contributes to the malignant transformation of NK-cells.

To further understand the basis of the functional changes induced by *PRDM1* KO, we compared the gene expression profiles of *PRDM1*$^{-/-}$ and WT NK-cell clones. As expected, there was a higher level of MYC and activation of the MYC signature with the loss of *PRDM1*, since *MYC* is a direct target of PRDM1. Many proliferation- and cell cycle-related pathways were highly enriched, including upregulation of many genes regulated by the DREAM complex. Signatures associated with IL-6, IL-15 and IL-2 stimulation were enriched, indicating that functional activities related to these cytokines are normally repressed by PRDM1. Similarly, TCR/NK-cell signaling was negatively regulated in WT cells compared with KO cells, indicating that removal of PRDM1 facilitates activation of these pathways. Additional mechanisms may contribute to driving the cell cycle, proliferation and survival, including the downregulation of the pro-apoptotic factor BIM and the upregulation of additional factors such as *TLR4, TOX2, CCR4, VGEFA, MYB, BCAT1, FGFR1* and *SIPR1*. We repeated the experiments with another gene editing approach without subsequent cloning and obtained similar

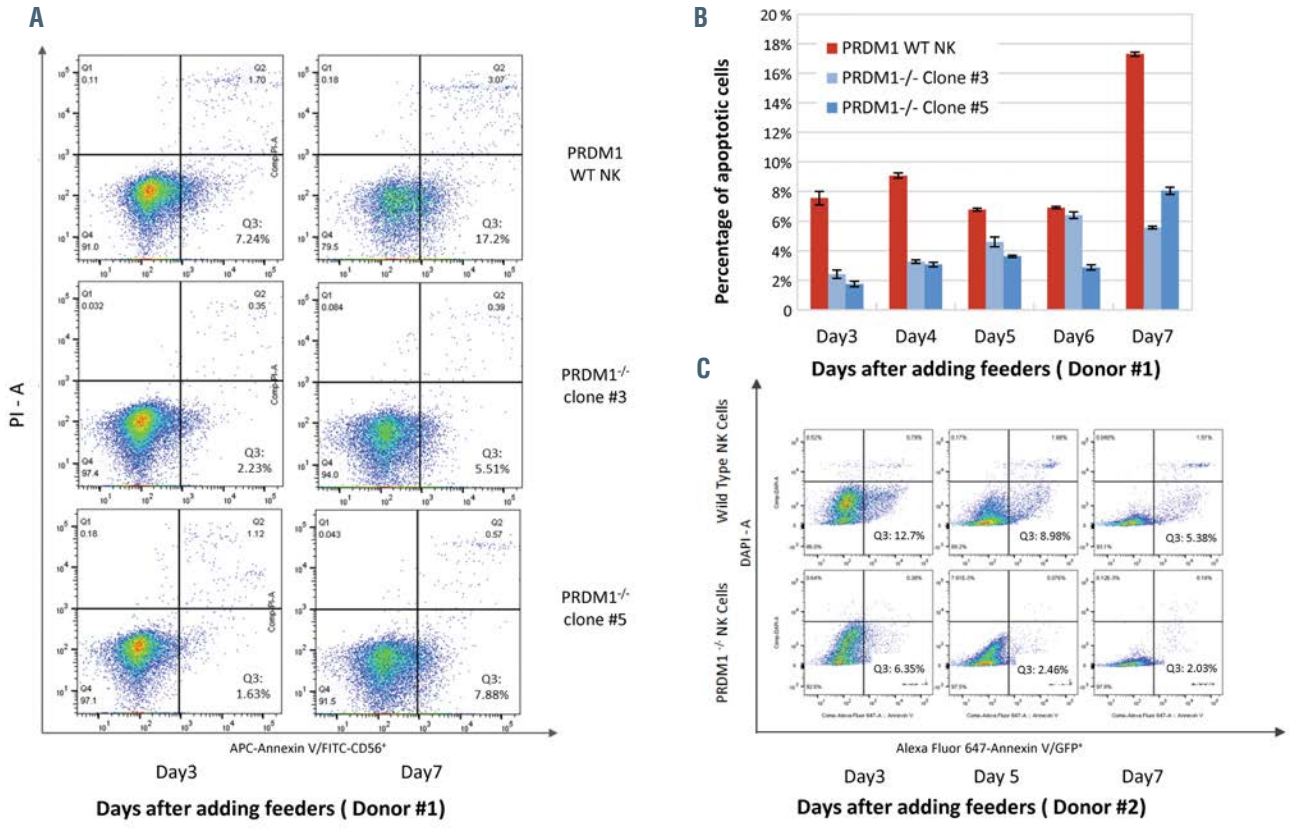

Figure 6. Apoptosis of *PRDM1*$^{-/-}$ NK cells *versus* wild-type NK cells. Apoptotic cells were analyzed with annexin V/propidium iodide (or DAPI) staining and a flow cytometry assay. Numbers in Q3 (percentage of APC or Alexa Fluor 647 annexin V-positive and propidium iodide- or DAPI-negative cells) were considered the early apoptotic cells. FITC anti-CD56 antibody staining was used to identify NK cells. Each staining was performed in duplicate. (A) Flow analysis of clones #3 and #5 from NK cells (donor #1) on day 3 and day 7 after addition of feeder cells. (B) Statistical analysis of the average percentage. (C) Experiments were repeated on NK cells (donor #2) edited by Cas9/sgRNA RNP plus homology directed repair. GFP positivity for *PRDM1*$^{-/-}$ cells and FITC CD56 positivity to identify NK cells.

results, supporting the validity of the findings. Thus, the loss of *PRDM1* altered the transcriptome with upregulation of *MYC, MYB* and many pathways associated with growth and proliferation, including those associated with cytokine stimulation and receptor signaling. On the other hand, pathways associated with normal cellular functions including cytotoxic functions were down-regulated, suggesting that the loss of *PRDM1* shifted the cell toward proliferation and survival rather than the performance of its normal effector function. The loss of immune checkpoint molecules may be more relevant in the *in vivo* setting, in which the cells may be able to escape from extrinsic controls, and could be relevant to lymphomagenesis.

CRISPR/Cas9 may generate off-target modifications that could potentially compromise our data and interpretation. We examined a number of clones for mutations using a custom capture platform (*Online Supplementary Table S5*) with an extensive set of genes known to harbor lymphoma-associated mutations and did not observe any mutations in these genes. The observation suggested that the CRISPR/Cas9 modifications did not induce off-target mutations of known oncogenic drivers and that our observations in the *PRDM1* KO cells were likely *PRDM1*-specific. Our approach cannot exclude the editing of genetic loci not examined. Therefore, we used a different approach to generate KO NK cells from different donors, with different guide RNA, and without subsequent cloning. Since off-target editing is unlikely to be the same in different cells and with a different guide RNA, critical findings were confirmed in our second approach with modification of a bulk population.

One of our long-term goals is to study cooperative effects of two or more mutations. With the *PRDM1*-deleted background, we were able to generate double mutant (i.e. *PRDM1*$^{-/-}$*/TP53*$^{+/-}$, *PRDM1*$^{-/-}$*/DDX3X*$^{+/-}$, and *PRDM1*$^{-/-}$*/PTPN6*$^{+/-}$) clones successfully using the plasmid/cloning approach. The growth of the NK cells started to slow down after prolonged *in vitro* culture. Therefore, to accelerate the experiments and to reduce secondary changes that may accumulate in prolonged culture, we tested the feasibility of simultaneously editing multiple genes in NK cells. Although it is feasible to modify two genes simultaneously, modifying three genes simultaneously was very inefficient using our current approach, probably partly because the cell cannot tolerate multiple double-stranded DNA breaks. Using the plasmid CRISPR/Cas9 KO strategy, we have only isolated heterozygous deleted clones, but with the current, more efficient Cas9/sgRNA RNP electroporation procedure, besides inserting a fluorescent protein gene in one allele, 70% of the other alleles were also modified by indels as analyzed by an online software ICE (Synthego, CA, USA) (*Online Supplementary Figure S10*). This suggested a more promising homozygous gene editing by the RNP electroporation method. The CRISPR/Cas9 technology is rapidly advancing, and innovative approaches can be incorporated in the future as they appear.

While the loss of function of *PRDM1* is frequent[5,6] and likely to be one of the early alterations in the development

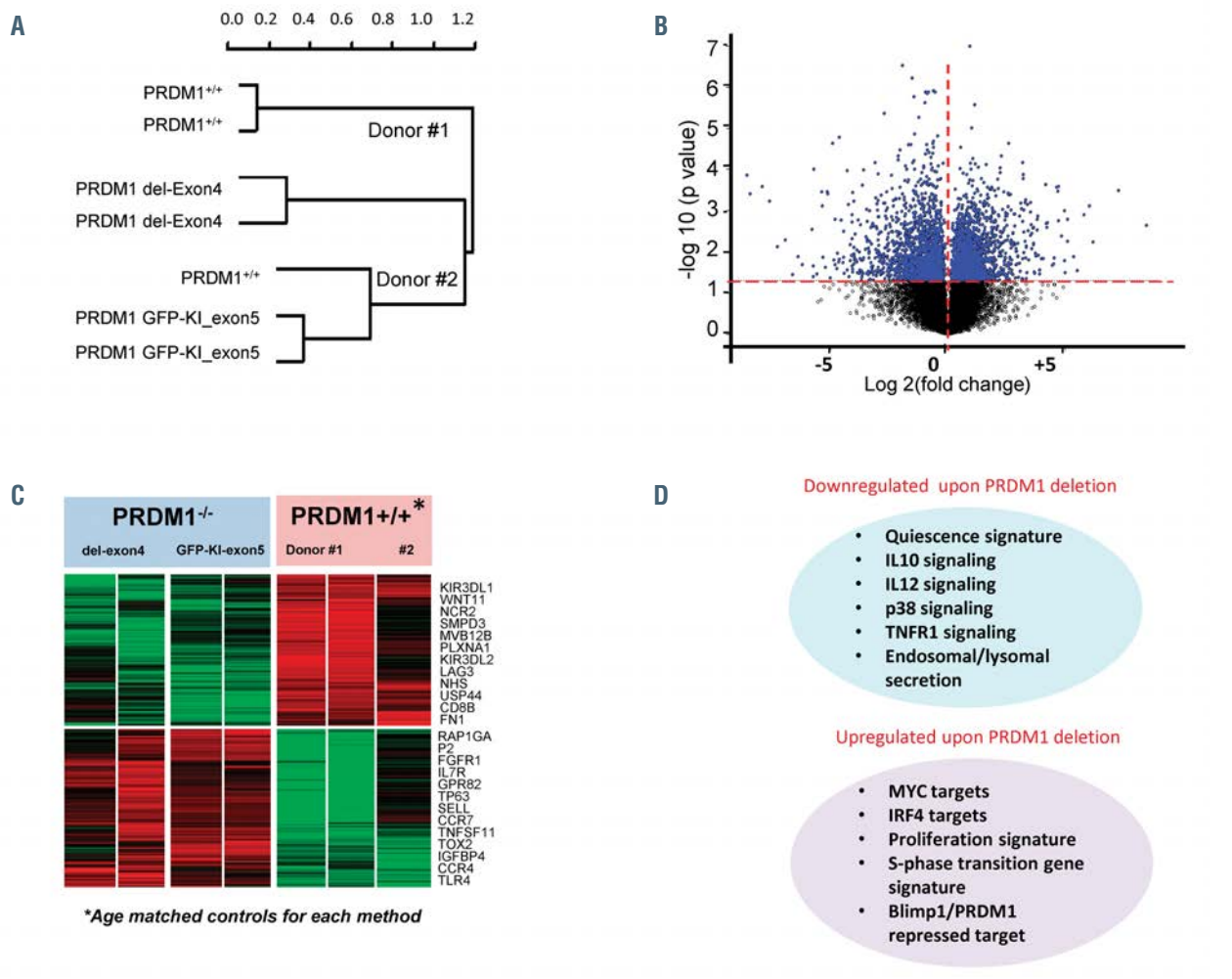

Figure 7. RNA-sequencing analysis of *PRDM1*$^{-/-}$ cells *versus* wild-type NK cells. (A) Unsupervised clustering of gene expression profiling data of *PRDM1* knock-out clones and cell age-matched parental wild-type NK cells. (B) Volcano plot of the differentiated transcriptional profile between *PRDM1*$^{-/-}$ and *PRDM1*$^{+/+}$ NK cells. (C) Heatmap of genes differentially expressed between *PRDM1*$^{-/-}$ and *PRDM1*$^{+/+}$ NK cells. (D) Summary of gene set enrichment analysis.

of NK-cell malignancies, it probably occurs after EBV infection of the NK cells. The ideal NK-cell lymphoma model may need to be derived from EBV-infected NK cells. We have not been successful in obtaining a viable expanding population of EBV-infected WT or *PRDM1* KO cells using EBV from Akata cells as reported.[33,34] Further studies will need to be performed to find the appropriate conditions and developmental stage of NK cells for EBV infection and persistence.

In summary, we have reported a disease modeling approach through the introduction of a tumor-driving mutation into normal NK cells through genetic editing. We examined the functional consequences of *PRDM1* deletion and elucidated the major pathways through which PRDM1 mediates its homeostatic control of NK cells. The recent development of CRISPR/Cas9 and long-term culture technologies enables selected lesions to be introduced singly or in combination into normal human NK cells. Associated functional alterations can then be assessed in the absence of the noise arising from the many other abnormalities present in tumor samples. This provides a powerful approach to dissect oncogenic interactions, thereby facilitating our understanding of the mechanistic basis of their cooperativity in oncogenesis. Future development of the technology will improve the range, speed and specificity of genetic editing, making this a feasible approach for studying functional changes resulting from a combination of oncogenic events and the essential changes necessary in the generation of a lymphoma. This approach can be applied to the study of T- and B-cell lymphomas and is particularly valuable in the study of tumors for which authentic cell lines or animal models are not available.

Disclosures

No conflicts of interest to disclose.

Contributions

GD and WCC conceived and designed the project; GD, YL and LL performed the NK-cell cloning, CRISPR experiments, and KO cell functional studies; XuL, YS and XiL performed the expression level assay and cell maintenance; CL helped with the CRISPR sgRNA design and HDRT construction; LK helped with the plasmid construction and identification of KO clones; JW performed RNA-sequencing experiments; AB, JI, QG and TWM analyzed the data; GD, YL, JI and WCC wrote and finalized the manuscript.

Acknowledgments

We thank Dr. Dean A. Lee, MD, PhD (Division of Hematology/Oncology/BMT, Nationwide Children's Hospital,

Columbus, OH, USA) for providing us feeder cells for NK-cell stimulation and Ni Feng and Lucy Brown from the City of Hope Analytical Cytometry Core (Duarte, CA, USA) for flow cytometric sorting. Research reported in this publication also included work performed in the Integrative Genomics Core and Gene Editing and Viral Vector Core in City of Hope.

Funding

This project was supported in part by the National Cancer Institute of the National Institutes of Health under grant number P30CA033572. It was also partly supported by the Dr. Norman and Melinda Payson Professorship in Hematologic Cancers and Tony Stephenson Lymphoma Center of City of Hope.

References

1. Yang Y, Cao JZ, Lan SM, et al. Association of improved locoregional control with prolonged survival in early-stage extranodal nasal-type natural killer/T-cell lymphoma. JAMA Oncol. 2017;3(1):83-91.
2. Li X, Cui Y, Sun Z, et al. DDGP versus SMILE in newly diagnosed advanced natural killer/T-cell lymphoma: a randomized controlled, multicenter, open-labelsStudy in China. Clin Cancer Res. 2016; 22(21):5223-5228.
3. Tse E, Kwong YL. Diagnosis and management of extranodal NK/T cell lymphoma nasal type. Expert Rev Hematol. 2016; 9(9):861-871.
4. Boi M, Zucca E, Inghirami G, Bertoni F. PRDM1/BLIMP1: a tumor suppressor gene in B and T cell lymphomas. Leuk Lymphoma. 2015;56(5):1223-1228.
5. Kucuk C, Hu X, Jiang B, et al. Global promoter methylation analysis reveals novel candidate tumor suppressor genes in natural killer cell lymphoma. Clin Cancer Res. 2015;21(7):1699-1711.
6. Kucuk C, Iqbal J, Hu X, et al. PRDM1 is a tumor suppressor gene in natural killer cell malignancies. Proc Natl Acad Sci U S A. 2011;108(50): 20119-20124.
7. Karube K, Nakagawa M, Tsuzuki S, et al. Identification of FOXO3 and PRDM1 as tumor-suppressor gene candidates in NK-cell neoplasms by genomic and functional analyses. Blood. 2011;118(12):3195-3204.
8. Iqbal J, Kucuk C, Deleeuw R, et al. Genomic analyses reveal global functional alterations that promote tumor growth and novel tumor suppressor genes in natural killer-cell malignancies. Leukemia. 2009;23(6):1139.
9. Boi M, Rinaldi A, Kwee I, et al. PRDM1/BLIMP1 is commonly inactivated in anaplastic large T-cell lymphoma. Blood. 2013;122(15):2683-2693.
10. Savage HP, Yenson VM, Sawhney SS, et al. Blimp-1-dependent and -independent natural antibody production by B-1 and B-1-derived plasma cells. J Exp Med. 2017;214(9):2777-2794.
11. Cong L, Ran FA, Cox D, et al. Multiplex genome engineering using CRISPR/Cas systems. Science. 2013;339(6121):819-823.
12. Dobashi A, Tsuyama N, Asaka R, et al. Frequent BCOR aberrations in extranodal NK/T-cell lymphoma, nasal type. Genes Chromosomes Cancer. 2016;55(5):460-471.
13. Jiang L, Gu ZH, Yan ZX, et al. Exome sequencing identifies somatic mutations of DDX3X in natural killer/T-cell lymphoma. Nat Genet. 2015;47(9):1061-1066.
14. Lee S, Park HY, Kang SY, et al. Genetic alterations of JAK/STAT cascade and histone modification in extranodal NK/T-cell lymphoma nasal type. Oncotarget. 2015; 6(19):17764-17776.
15. Koo GC, Tan SY, Tang T, et al. Janus kinase 3-activating mutations identified in natural killer/T-cell lymphoma. Cancer Discov. 2012;2(7):591-597.
16. Sim SH, Kim S, Kim TM, et al. Novel JAK3-activating mutations in extranodal NK/T-cell lymphoma, nasal type. Am J Pathol. 2017;187(5):980-986.
17. Roth TL, Puig-Saus C, Yu R, et al. Reprogramming human T cell function and specificity with non-viral genome targeting. Nature. 2018;559(7714):405-409.
18. Ran FA, Hsu PD, Wright J, et al. Genome engineering using the CRISPR-Cas9 system. Nat Protoc. 2013;8(11):2281-2308.
19. Mian MF, Lauzon NM, Andrews DW, et al. FimH can directly activate human and murine natural killer cells via TLR4. Mol Ther. 2010;18(7):1379-1388.
20. Stolberg VR, Martin B, Mancuso P, et al. Role of CC chemokine receptor 4 in natural killer cell activation during acute cigarette smoke exposure. Am J Pathol 2014; 184(2):454-463.
21. Chen WS, Kitson RP, Goldfarb RH. Modulation of human NK cell lines by vascular endothelial growth factor and receptor VEGFR-1 (FLT-1). In Vivo. 2002; 16(6):439-445.
22. Vong QP, Leung WH, Houston J, et al. TOX2 regulates human natural killer cell development by controlling T-BET expression. Blood. 2014;124(26):3905-3913.
23. Kallies A, Carotta S, Huntington ND, et al. A role for Blimp1 in the transcriptional network controlling natural killer cell maturation. Blood. 2011;117(6):1869-1879.
24. Chihara N, Madi A, Kondo T, et al. Induction and transcriptional regulation of the co-inhibitory gene module in T cells. Nature. 2018;558(7710):454-459.
25. Kucuk C, Jiang B, Hu X, et al. Activating mutations of STAT5B and STAT3 in lymphomas derived from gammadelta-T or NK cells. Nat Commun 2015;6:6025.
26. El-Tayeb A, Iqbal J, Behrenswerth A, et al. Nucleoside-5'-monophosphates as prodrugs of adenosine A2A receptor agonists activated by ecto-5'-nucleotidase. J Med Chem. 2009;52(23):7669-7677.
27. Kucuk C, Hu X, Iqbal J, et al. HACE1 is a tumor suppressor gene candidate in natural killer cell neoplasms. Am J Pathol. 2013; 182(1):49-55.
28. Demosthenous C, Han JJ, Hu G, et al. Loss of function mutations in PTPN6 promote STAT3 deregulation via JAK3 kinase in diffuse large B-cell lymphoma. Oncotarget. 2015;6(42):44703-44713.
29. Sharma Y, Ahmad A, Bashir S, et al. Implication of protein tyrosine phosphatase SHP-1 in cancer-related signaling pathways. Future Oncol. 2016;12(10):1287-1298.
30. Yin S, Wu H, Lv J, et al. SHP-1 arrests mouse early embryo development through downregulation of Nanog by dephosphorylation of STAT3. PloS One 2014; 9(1):e86330.
31. Nakamura MC, Niemi EC, Fisher MJ, et al. Mouse Ly-49A interrupts early signaling events in natural killer cell cytotoxicity and functionally associates with the SHP-1 tyrosine phosphatase. J Exp Med. 1997; 185(4):673-684.
32. Mahmood S, Kanwar N, Tran J, et al. SHP-1 phosphatase is a critical regulator in preventing natural killer cell self-killing. PloS One. 2012;7(8):e44244.
33. Isobe Y, Sugimoto K, Yang L, et al. Epstein-Barr virus infection of human natural killer cell lines and peripheral blood natural killer cells. Cancer Res. 2004;64(6):2167-2174.
34. Isobe Y, Sugimoto K, Yang L, et al. Epstein-Barr virus infection of human natural killer cell lines and peripheral blood natural killer cells. Cancer Res. 2004;64(6):2167-2174.